Single-walled carbon nanotubes in superacid: X-ray and calorimetric evidence for partly ordered H_2SO_4

W. Zhou and J. E. Fischer*
Department of Materials Science and Engineering, University of Pennsylvania, Philadelphia, Pennsylvania 19104, USA

P. A. Heiney
Department of Physics and Astronomy, University of Pennsylvania, Philadelphia, Pennsylvania 19104, USA

H. Fan, V. A. Davis, M. Pasquali, and R. E. Smalley
Center for Nanoscale Science and Technology, Rice University, Houston, Texas 77005, USA
(Received 7 February 2005; published 18 July 2005)

Liquid anhydrous sulfuric acid forms a partly ordered structure in the presence of single-walled carbon nanotubes (SWNTs). X-ray scattering from aligned fibers immersed in acid shows the formation of molecular shells wrapped around SWNTs. Differential scanning calorimetry of SWNT-acid suspensions exhibits concentration-dependent supercooling/melting behavior, confirming that the partly ordered molecules are a new phase. We propose that charge transfer between nanotube π electrons and highly oxidizing superacid is responsible for the unique partly ordered structure.

DOI: 10.1103/PhysRevB.72.045440 PACS number(s): 61.48.+c, 81.07.De

Many theories and simulations predict "structured water" shells surrounding dissolved cations due to short-range hydration effects. Experimental evidence is sparse and indirect, and the concept is still debated.[1,2] Here we report unambiguous structural and thermodynamic evidence for partly ordered protic solvent molecules surrounding a molecular scale solute. Our solvent is anhydrous 102% sulfuric acid (2 wt. % excess SO_3) and the solute is single-walled carbon nanotubes (SWNTs).[3] We show that H_2SO_4 molecules readily intercalate SWNT ropes,[4] forming a partly ordered solvent structure wrapped around the tubes and tube ropes. Moreover, the solvent molecules associated with the nanotube solute exhibit different phase behavior compared to pure acid. We propose that charge transfer between nanotube π electrons and H_2SO_4 molecules is responsible for the formation of "structured acid" around the nanotubes.

We used well-aligned nanotube fibers[5] spun from purified HiPco SWNT for the x-ray scattering experiments. The major impurity was <1.2 at. % Fe residual catalyst particles. Most of the residual Fe was encapsulated in graphitic shells. Very little amorphous carbon was observed in transmission electron microscopy of similarly purified samples.[6] Graphite impurities are ubiquitous in SWNT produced by arc or laser ablation from graphite targets, while the HiPco process uses CO and $Fe(CO)_5$ as feedstock and catalyst, respectively.

Nanotube alignment within the oriented one-dimensional (1D) fiber assemblies was characterized by a Gaussian mosaic dispersion full width at half-maximum (FWHM) of 31.5°,[5] thus providing an excellent system in which to look for ordered solvent molecules around a solute. Three types of sample were studied. *Dry* fibers were vacuum-annealed at 1100 °C for 2 h to drive off impurities. About 25 fibers, ~5 mm in length and ~40 μm in diameter, were packed into 0.5 mm glass capillaries, carefully maintaining the fibers parallel to the axis of the capillary. *Swollen* fibers were prepared as above by adding anhydrous sulfuric acid to the capillary. The density of dry fiber is ~1.1 g/cm^3 and thus contains ~30 vol. % voids[5] since the ideal density of an (8, 8) nanotube crystal is ~1.5 g/cm^3 [we take (8, 8) as representative of the ~11 Å mean diameter of HiPco tubes]. These dry fibers immersed in sulfuric acid swell by 30%–60% in diameter upon reimmersion.[5] A *control* sample of pure acid was also measured. All sample preparations involving acid were carried out in a dry box, with only brief exposure to air when the capillaries were sealed off.

X-ray experiments employed Cu K_α radiation from a rotating anode source, doubly focusing optics, evacuated flight path, and two-dimensional (2D) wire detector.[7] All samples were measured in transmission for 2 h with the fiber axis perpendicular to the incident beam. Scattering from an empty capillary was subtracted. Figure 1(a) shows the detector image for the dry fiber (inset) along with the scattering profiles (intensity vs wave vector Q) obtained by azimuthal integration of the 2D data over the full circle. Figure 1(b) presents the same information for the swollen fiber and the control sample, and Fig. 1(c) gives azimuthal variation of intensity at fixed Q for dry and swollen fibers. These were obtained for the dry sample (top) by averaging pixels in the range $0.4 < Q < 0.6$ Å^{-1} which straddles the (10) reflection of the triangular lattice,[4] and for the swollen sample (bottom) by averaging pixels in the range $1.1 < Q < 1.9$ Å^{-1} which straddles the first peak in the acid scattering profile. Mosaic FWHM's are both ~32°, a surprising result discussed in detail below.

The 2D pattern from dry fibers has two components. Intense Bragg reflections with azimuthal preferred orientation are attributed to the aforementioned aligned SWNTs in semicrystalline ropes, while strong small-angle x-ray scattering (SAXS) diffuse intensity is assigned to the structural inhomogeneity on large length scales (aligned ropes vs voids between ropes),[8] discussed in detail below. The dotted line in Fig. 1(a) is a simulated profile of just the Bragg scattering,[4] assuming an average tube diameter of 11.2 Å and a Gaussian diameter distribution with 2 Å FWHM. It reproduces the Bragg reflections very well.

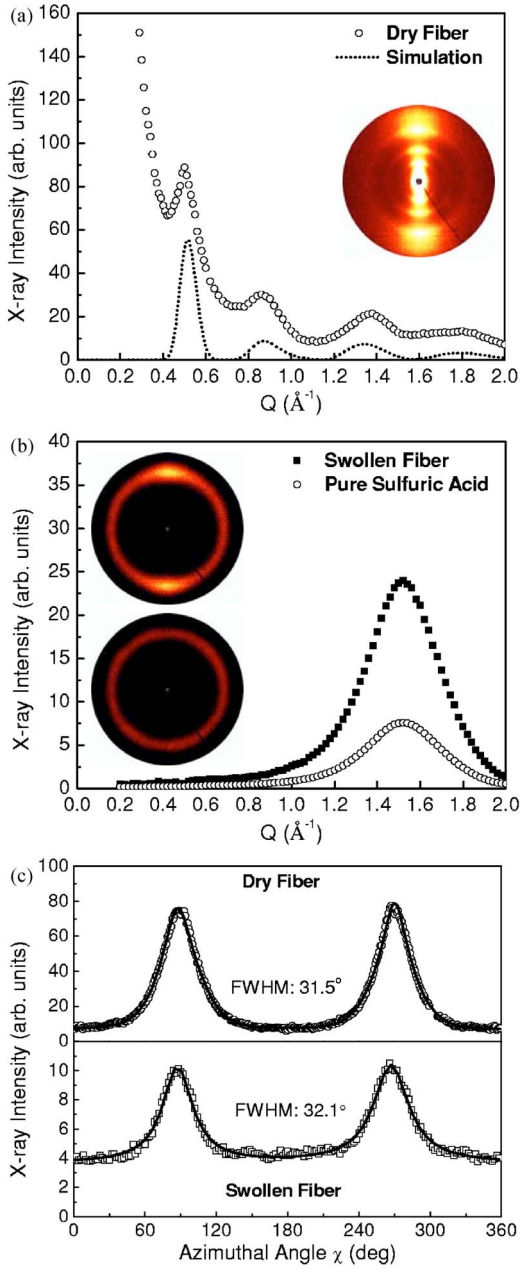

FIG. 1. (Color online) X-ray scattering data. (a) Integrated scattering profile (empty circles) of dry annealed SWNT fibers. Model calculations (dotted line) assuming a mean diameter of 11.2 Å reproduce the Bragg peaks very well. Inset is the 2D detector false-color image. (b) Same for swollen fiber in acid (solid squares) and pure acid (empty circles). Scattering from acid is enhanced and anisotropic in the presence of fibers, and SWNT ropes are no longer detectable. (c) Azimuthal intensity variations of the (10) rope Bragg peak at $Q=0.5$ Å^{-1} from dry fiber (top), and of the first order diffuse scattering at $Q=1.5$ Å^{-1} from acid in which the swollen fiber is immersed (bottom); the mosaic FWHM's are the same ($\sim 32°$) within experimental error.

For the swollen fibers, Fig. 1(b), both SAXS and Bragg intensities are greatly diminished; measurements down to $Q\sim 0.01$ Å^{-1} confirmed that the SAXS intensity is essentially zero. Transmission through the acid+capillary is $>30\%$, ruling out absorption as the origin of the disappearance of SAXS and Bragg intensities.

Small-angle x-ray scattering originates from inhomogeneity of the charge distribution on length scales large compared to interatomic spacings, for example, the "contrast," or difference in scattering power, between a low-density medium and dense scatterers or between a compact dense medium and internal voids. For a two-phase material with uncorrelated inhomogeneities, the SAXS intensity is proportional to the square of the electron scattering length density difference between the two homogeneous phases (SLD, unit: 10^{-5} Å^{-2}).[9] Here in dry SWNT fibers, the two phases are the SWNT ropes and the voids between ropes ($\sim 30\%$ of the total volume), respectively. For swollen fibers immersed in acid, all voids are filled with acid, and thus the two phases are the SWNT ropes and bulk acid. The calculated SLD's of sulfuric acid and our SWNT ropes are 1.64 and ~ 1.29, respectively,[10] and the SLD of free space is zero. Simply filling with acid the voids between ropes would not explain the diminished SAXS intensity since the average contrast between ropes and acid would still be ~ 0.35 (assuming that the ropes were unaltered by acid). The absence of SAXS intensity after swelling is more likely due to some combination of (a) sulfuric acid intercalating the ropes such that the average SLD of the ropes increases to the acid value, and (b) rope swelling decreasing the void volume fraction. The former is strongly supported by the observation that swollen fibers sink in the acid.[5] The mass densities of dry fiber (~ 1.1 g/cm^3) and crystalline (8, 8) nanotube rope (~ 1.5 g/cm^3) are both significantly smaller than that of sulfuric acid (~ 1.9 g/cm^3). The increase of electron SLD is consistent with the observed increase of mass density of nanotube ropes upon acid intercalation.

The Bragg reflections from the SWNT ropes also disappear after immersion, implying that H_2SO_4 molecules intercalate in a disordered manner which smears out the triangular lattice reflections. This is similar to what occurs during electrochemical intercalation of SWNT with alkali metals.[11] The dilation or "fraying" of ropes by acid immersion is analogous to reversible disruption of the triangular lattice by coinsertion of electrolyte solvent molecules which partially solvate the intercalated cations. The general phenomenon of solvated intercalates is well known in graphite intercalation compounds.[12]

Most striking in Fig. 1(b) is the strongly enhanced and anisotropic 2D scattering from the acid. H_2SO_4 is a highly associated liquid; its short-range structure closely resembles that of the structure in the corresponding condensed phase.[13] Solid H_2SO_4 has a layered structure with hydrogen bonding only within layers. The layer-layer separation is ~ 4.02 Å. The liquid can be envisioned as small clusters with a similar layered motif.[13] Our control sample shows an azimuthally featureless diffuse band of isotropic scattering centered at $Q\sim 1.5$ Å^{-1}, consistent with previous results.[13] Note that this Q differs significantly from the nearest rope peaks, cf. Fig. 1(a), and is thus unambiguously assigned to liquid acid. In sharp contrast, acid diffuse scattering from the swollen fiber+acid sample is strongly anisotropic and much more intense than that of the control sample. The mosaic FWHM is the same as that of ropes in the dry fiber. This means that

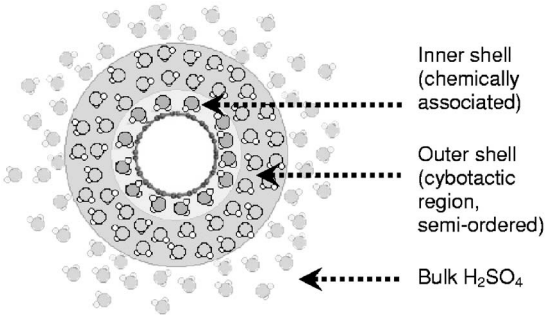

FIG. 2. Schematic showing the cross section of a SWNT or a rope wrapped in cylindrical shells of sulfuric acid.

some fraction of the liquid clusters are aligned along the fiber axis, forming shells wrapped around tubes and ropes. A hypothetical structure which would explain oriented diffuse acid scattering is shown in Fig. 2. The FWHM of the acid scattering is the same as that of the ropes in the dry fiber because the orientations of the shells are determined by those of the SWNTs in the fibers. Enhanced acid scattering intensity from the swollen fiber also originates from the partly ordered H_2SO_4 shells. In the control sample, the scattering is distributed over a spherical shell in reciprocal space. Conversely, in the oriented fiber+acid sample the acid scattering is distributed over a cylindrical annulus aligned with the fibers, and is thus more concentrated in cylindrical mosaic arcs compared to a "perfect powder" diffuse sphere. Therefore, the integrated intensity in the plane of our 2D x-ray detector increases for aligned samples while the total intensity integrated over 4π steradians remains the same as in a totally random sample.

We estimate the number of acid layers in a shell using relative x-ray intensities and volume fractions of various species present in the capillary. Free acid outside the swollen fibers, acid inside the swollen fibers and SWNT occupy ~45%, ~35%, and ~20%, respectively, of the capillary cross-sectional area, as determined from the fiber diameter (~40 μm), void fraction (~30%), the number of fibers (25), fiber swelling ratio (~1.3–1.6) and the capillary diameter (~500 μm). From the texture of the acid, Fig. 1(c), we estimate that ~1/3 of the total volume is oriented. This suggests that most of the acid within the fiber is aligned and that each tube is wrapped with 2 to 3 molecular layers on average. However, since the whole fiber swells only by ~1.3–1.6 in diameter, the possible number of acid layers surrounding each tube in a rope can be approximately one to two at most. This means that the acid on the rope surface or isolated tube surface must be more than two to three layers. Therefore, the anisotropic x-ray scattering is mainly from the acid shells surrounding ropes or isolated tubes, and not primarily from acid in the intercalated ropes. The detailed structure of the disordered intercalated ropes is unclear, but certainly an interesting topic for further study.

The x-ray analysis clearly suggests that in the presence of nanotubes, some fraction of the acid becomes associated with the SWNT, leading to partial order. This acid should represent a phase different from bulk acid, for example, having slightly different local density (which we were unable to

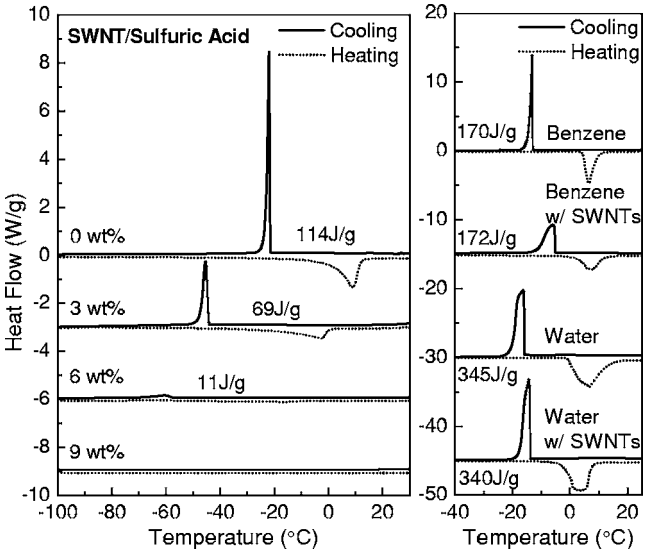

FIG. 3. Differential scanning calorimetry data. Left, SWNT dispersion in sulfuric acid. Right, benzene (top) or water (bottom) with and without SWNTs. Enthalpies of the phase transition are normalized to "J/gram of solvent." SWNTs dramatically affect the phase transition of sulfuric acid, suggesting the presence of a acid phase associated with SWNT. In contrast, SWNT have no significant effect on the phase transitions of benzene or water.

detect from the diffuse scattering). To test this conjecture we performed differential scanning calorimetry (DSC, TA Instruments Model 2920, 5 °C/min) on SWNT dispersions of different concentrations in anhydrous sulfuric acid. Samples were hermetically sealed in aluminum pans lined with gold foil, inside a dry box. The results are shown in Fig. 3. Acid alone shows a strong sharp crystallization peak upon cooling, and a melting peak upon heating with an enthalpy of ~114 J/g, close to that of 100% sulfuric acid (109 J/g). With increasing SWNT concentration, the melting point and enthalpy both decrease, strongly suggesting the presence of two types of acid in the suspensions. Free acid behaves similarly to pure bulk acid and will crystallize and melt with concentration-dependent shifts in temperatures due to the dissolved SWNT. Conversely, the partly ordered acid associated with nanotubes does not crystallize or melt in the temperature range investigated; its *properties* would be expected to be independent of SWNT concentration as long as sufficient global acid were present in the capillary.

On the other hand, the *volume fraction* of partly ordered acid increases with increasing SWNT concentration. At low concentration, most of the acid is free. At 3 wt % for this sample, we deduce that ~60% of the acid is free, from the reduction in enthalpy per acid mass, 69 J/g vs 114 J/g. At 6 wt % SWNT there remains less than 10% free acid, while at 9 wt % almost all available acid molecules are associated with nanotubes. This progression agrees well with rheological results[14] which suggest that below ~4 wt %, an isotropic solution phase coexists with a nematic liquid crystal (LC) phase, while suspensions with higher concentration are dominated by the LC phase. The enthalpy/concentration correlation is also consistent with the x-ray results which suggest that nearly all the acid in the swollen fiber is partly

ordered (the weight ratio of nanotubes to acid in the swollen fiber is ~1:2 while it is ~1:10 in the most concentrated dispersion).

Unfortunately the x-ray and calorimetry data do not provide specific chemical information about nanotube-sulfuric acid interactions. We propose that charge transfer between nanotube pseudo-π states and H_2SO_4 molecules is the driving force for acid intercalation, and for the unique partly ordered H_2SO_4 structure around nanotubes. To support this proposal, we compare H_2SO_4 suspensions with benzene- and water-SWNT mixtures. SWNTs have no specific strong interactions with C_6H_6 or H_2O, and both are very weak charge donors to nanotubes.[15]

Fibers sealed in capillaries with benzene or water do not swell after weeks. The insets in Fig. 4 show detector images differing dramatically from that of the swollen fiber+acid sample, Fig. 1(b). The nanotube scattering does not disappear and resembles that of the dry fiber. Evidently the amount of benzene/water entering or intercalating nanotube ropes is quite small. Moreover, scattering from the solvent is not anisotropic. This is more clearly demonstrated in the profiles shown in Fig. 4, which are azimuthal integrations of the 2D data 60° wide in χ centered at 90° and 180°. The difference represents the scattering from the fiber and any possible ordered structure of solvent wrapped around tubes or ropes. The difference profile is nearly the same as that of the dry fiber and contains no hint of extra scattering from the solvents. (The "hot spots" in the detector image arise from the superposition of nanotube and solvent scattering.) We see no evidence for cylindrical shells of benzene or water around nanotube ropes, the van der Waals interaction between benzene/water molecules and SWNT surfaces being far too weak.

DSC measurements confirm that there are no additional phases associated with SWNT in ordinary solvents. 20 wt % nanotubes were mixed with benzene or water to form pastes which were sealed in Al pans. The data on the right-hand panel of Fig. 3 show that, aside from minor changes in transition temperature (possibly due to adsorption effects and/or porosity), the enthalpy does not change. Thus, nanotubes have no significant effect on the freezing and melting of water or benzene, as expected.

In summary, we used x-ray scattering from fibers of well-oriented SWNT to identify partly ordered solvent molecules surrounding a molecular scale solute in a hydrogen-bonded system. Acid molecules intercalate into ropes and form cylindrical shells wrapped around nanotubes and/or ropes. DSC confirms that the partly ordered acid associated with nanotubes is a different phase from bulk acid. Highly oriented solvent molecules have been previously observed in a rodlike polymer/polyphosphoric acid solution, as part of a study focusing on a crystal solvate phase.[16] Partly ordered structures should also exist for SWNT in other superacids (chlorosulfonic acid, triflic acid, etc.). All of these can be thought of as superionic surfactants from the standpoint of separating

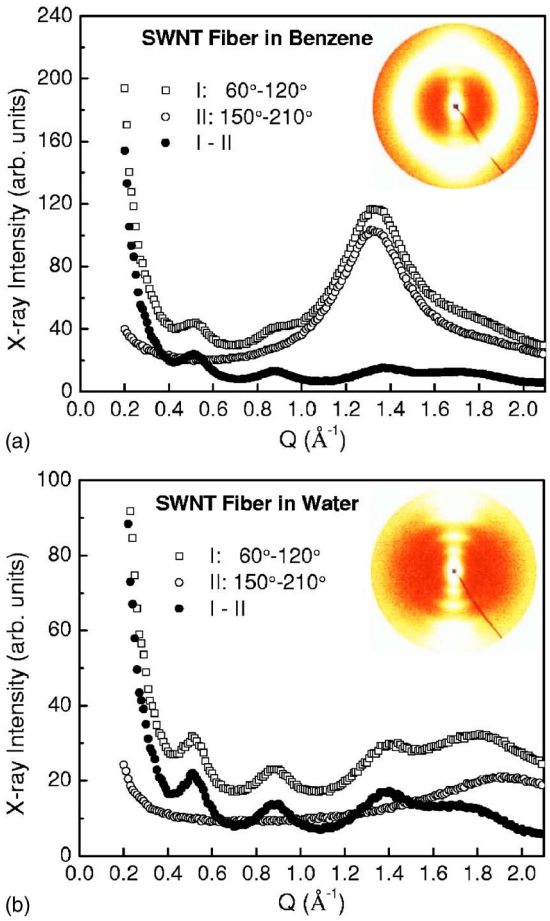

FIG. 4. (Color online) X-ray scattering data from SWNT fibers in benzene (a) or water (b). Insets are 2D detector false-color images. Azimuthal integrations of the 2D data 60° wide in χ centered at 90° (I, empty squares) and 180° (II, empty circles) are shown. The difference (I–II, solid circles), which would expose an ordered structure of solvent wrapped around SWNT, shows only Bragg peaks from SWNT ropes. The absence of excess solvent scattering proves the absence of ordered solvent phases associated with SWNT.

and isolating SWNT and ropes. We find no evidence for ordered or aligned molecules once the superacids are exposed to water. Presumably this is due to the high affinity of H_2O for H_2SO_4 and the diminished oxidizing power of the diluted solvent.[17] Partly ordered structures were not observed using ordinary solvents (H_2O, benzene, etc.) which have no strong interaction with nanotubes. The mechanism of charge transfer as the driving force for partly ordered acid shells is also supported by the observation of strongly metallic behavior in acid-doped SWNT.[8,18]

We acknowledge helpful discussions with M. L. Klein and A. R. McGhie. This work was supported by ONR under the DURINT program, Grant No. N00014-01-1-0789 and by ONR Grant No. N00014-03-1-0890 and by NSF Grant No. DMR-0102459.

*Electronic mail: fischer@seas.upenn.edu

[1] G. A. Krestov, *Thermodynamics of Solvation* (Ellis Horwood, Chichester, UK, 1991).

[2] A. W. Omta, M. F. Kropman, S. Woutersen, and H. J. Bakker, Science **301**, 347 (2003).

[3] S. Ramesh, L. M. Ericson, V. A. Davis, R. K. Saini, C. Kittrell, M. Pasquali, W. E. Billups, W. W. Adams, R. H. Hauge, and R. E. Smalley, J. Phys. Chem. B **108**, 8794 (2004).

[4] A. Thess, R. Lee, P. Nikolaev, H. Dai, P. Petit, J. Robert, C. Xu, H. Lee, S. G. Kim, D. T. Colbert, G. Scuseria, D. Tomanek, J. E. Fischer, and R. E. Smalley, Science **273**, 483 (1996).

[5] L. M. Ericson, H. Fan, H. Q. Peng, V. A. Davis, W. Zhou, J. Sulpizio, Y. H. Wang, R. Booker, J. Vavro, C. Guthy, A. N. G. Parra-Vasquez, M. J. Kim, S. Ramesh, R. K. Saini, C. Kittrell, G. Lavin, H. Schmidt, W. W. Adams, W. E. Billups, M. Pasquali, W. F. Hwang, R. H. Hauge, J. E. Fischer, and R. E. Smalley, Science **305**, 1447 (2004).

[6] W. Zhou, Y. H. Ooi, R. Russo, P. Papanek, D. E. Luzzi, J. E. Fischer, M. J. Bronikowski, P. A. Willis, and R. E. Smalley, Chem. Phys. Lett. **350**, 6 (2001).

[7] See http://www.lrsm.upenn.edu/lrsm/facMAXS.html for a description of the x-ray facility. The x-ray data were analyzed using Datasqueeze, http://www.datasqueezesoftware.com

[8] W. Zhou, J. Vavro, C. Guthy, K. I. Winey, J. E. Fischer, L. M. Ericson, S. Ramesh, R. Saini, V. A. Davis, C. Kittrell, M. Pasquali, R. H. Hauge, and R. E. Smalley, J. Appl. Phys. **95**, 649 (2004).

[9] L. A. Feigin and D. I. Svergun, in *Structure Analysis by Small-Angle X-ray and Neutron Scattering*, edited by G. W. Taylor (Plenum, New York, 1987).

[10] Calculations were done using a NIST program, http://www.ncnr.nist.gov/resources/sldcalc.html. SLD's of tubes and acid were constructed from known atomic values calculated, chemical composition and mass densities. Calculated SLDs are 1.14, 1.30, and 1.50 for (10, 10), (8, 8), and (6, 6) ropes, respectively. Parameters used, (10, 10) rope (tube diameter, d, 13.6 A; mass density, ρ, 1.34 g/cm^3), (8, 8) rope (d, 10.8 A; ρ, 1.53 g/cm^3), and (6, 6) rope (d, 8.1 A; ρ, 1.76 g/cm^3).

[11] A. S. Claye, J. E. Fischer, C. B. Huffman, A. G. Rinzler, and R. E. Smalley, J. Electrochem. Soc. **147**, 2845 (2000).

[12] J. R. Dahn, Phys. Rev. B **44**, 9170 (1991).

[13] C. Andreani, C. Petrillo, and F. Sacchetti, Mol. Phys. **58**, 299 (1986).

[14] V. A. Davis, L. M. Ericson, A. N. G. Parra-Vasquez, H. Fan, Y. H. Wang, V. Prieto, J. A. Longoria, S. Ramesh, R. K. Saini, C. Kittrell, W. E. Billups, W. W. Adams, R. H. Hauge, R. E. Smalley, and M. Pasquali, Macromolecules **37**, 154 (2004).

[15] J. Zhao, J. Han, and J. P. Lu, Appl. Phys. Lett. **82**, 3746 (2003).

[16] Y. Cohen, Y. Saruyama, and E. L. Thomas, Macromolecules **24**, 1161 (1991).

[17] G. U. Sumanasekera, J. L. Allen, S. L. Fang, A. L. Loper, A. M. Rao, and P. C. Eklund, J. Phys. Chem. B **103**, 4292 (1999).

[18] J. Vavro, M. C. Llaguno, J. E. Fischer, S. Ramesh, R. K. Saini, L. M. Ericson, V. A. Davis, R. H. Hauge, M. Pasquali, and R. E. Smalley, Phys. Rev. Lett. **90**, 065503 (2003).